Complexes of Acridine and 9-Chloroacridine with I_2: Formation of Unusual I_6 Chains through Charge-Transfer Interactions Involving Amphoteric I_2

Elizabeth L. Rimmer,[b] Rosa D. Bailey,[a] Timothy W. Hanks,*[b] and William T. Pennington*[a]

Abstract: Acridine and 9-chloroacridine form charge-transfer complexes with iodine in which the nitrogen-bound I_2 molecule is amphoteric; one end serves as a Lewis acid to the heterocyclic donor, while the other end acts as a Lewis base to a second I_2 molecule that bridges two acridine $\cdot I_2$ units. In the acridine derivative [(acridine $\cdot I_2)_2 \cdot I_2$, **1**], the dimer has a "zigzag" conformation, while in the 9-chloroacridine derivative [(9-Cl-acridine $\cdot I_2)_2 \cdot I_2$, **2**], the dimer is "C-shaped". The thermal decomposition of the two complexes is very different. Compound **1** loses one molecule of I_2 to form an acridine $\cdot I_2$ intermediate, which has not been isolated. Further decomposition gives acridine as the form **II** polymorph, exclusively. Decomposition of **2** involves the loss of two molecules of I_2 to form a relatively stable intermediate [(9-Cl-acridine$)_2 \cdot I_2$, **3**]. Compound **3** consists of two 9-Cl-acridine molecules bridged through N $\cdots$ I charge-transfer interactions by a single I_2 molecule. This compound represents the first known example, in which both ends of an I_2 molecule form interactions in a complex that is not stabilized by the extended interactions of an infinite chain structure. The ability of the terminal iodine of an N-bound I_2 to act either as an electron donor (complexes **1** and **2**) or as an electron acceptor (complex **3**) can be understood through a quantum mechanical analysis of the systems. Both electrostatic interactions and the overlap of frontier molecular orbitals contribute to the observed behavior.

Keywords: acridines · charge transfer · polymorphism · supramolecular chemistry

Introduction

There is currently intense interest in the systematic engineering of crystalline organic solids, in which careful control of the packing arrangements of the individual components leads to desirable macroscopic properties.[1] While the successful construction of a particular supramolecular motif is by no means trivial or routine, the need for such materials in areas as diverse as photonics or pharmaceuticals is nucleating a variety of interesting approaches. A major conceptual advance in the field that is assisting these activities is the extension of Corey's classical organic synthesis term of "synthons"[2] to supramolecular systems. While Corey was interested in reoccurring patterns in the construction of molecular species, Gautam Desiraju has redefined the term to refer to identifiable design elements, derived from specific combinations of *intermolecular* interactions.[3] If one develops an understanding of how to manipulate these "supramolecular synthons", the rational design of a variety of novel and valuable materials becomes feasible.

The most widely researched supramolecular synthons investigated to date are those involving hydrogen bonding.[4] The strength of this well-understood interaction often dominates the organization of crystalline organic solids. While this is a powerful tool, it is not ubiquitous and must be viewed as only one of many that are available. Full utilization of a wide array of methodologies will be required for future crystal engineering projects, and an active search for other identifiable families of interactions is proceeding. One promising area involves those interactions arising from "charge-transfer" between electron-rich and electron-poor molecular species. Charge-transfer interactions that involve donation of a lone-pair of electrons from a donor atom (such as nitrogen, phosphorus, or sulfur) into a σ* orbital of an acceptor atom (such as the halogens) are, like hydrogen bonds, selective, reasonably strong (approximately 10 kJ mol^{-1}), and highly directional.[5] They typically occur along lines of maximum probability for lone-pair localization on the donor atom and *trans* to σ-bonds of the acceptor atom. From the beginning with the seminal work of Mulliken,[6] these interactions have been widely investigated.[7]

[a] Prof. W. T. Pennington, R. D. Bailey
Department of Chemistry, Hunter Laboratories
Clemson University, Clemson, SC 29634-0973 (USA)
E-mail: billp@clemson.edu

[b] Prof. T. W. Hanks, E. L. Rimmer
Department of Chemistry, Furman University
Greenville, SC 29613 (USA)

  0947-6539/00/0622-4071 $ 17.50+.50/0

Crystal engineering applications have made use of chlorine-, bromine-, and iodine-containing acceptors.[8] We have focused on the latter, especially in conjunction with donors that feature nitrogen heterocycles.[9] Not only does the highly polarizable iodine form stronger interactions than the other halogens, it is also less prone to give side products due to oxidation of the donor (though this may still occur in certain situations). Our investigations of the N···I interaction have enabled us to define several associated supramolecular synthons. We are currently engaged in a long-term effort to thoroughly understand these synthons and to apply them towards the rational design of new and high-value materials.

Perhaps the most unique and potentially useful feature of crystal engineering with charge-transfer interactions of this type is that the resulting host–guest complexes are only metastable. In analogy with classical organic synthesis, one component of the charge-transfer complex (in our case, the Lewis acid component) may be considered to be a "protecting group" or even a "chiral auxiliary" in the sense that one of two (or more) similar reaction products may be selectively isolated after supramolecular assembly and removal of the acceptor subunit. For example, we have been able to use I_2 to control polymorph formation in the compound tetrapyridylpyrazine (tpp); we even converted the thermodynamically favored monoclinic form to the less favored tetragonal form entirely in the solid state.[10] This result is potentially of great industrial significance, particularly to pharmaceuticals, dyes, agrochemicals, explosives, and other industries, in which polymorphism can be critical to product performance. Related N···I interactions have been used to effect the separation of enantiomers[11] and to control the ability of diacetylenes to undergo solid-state polymerization.[12]

The observation that polymorphism can be controlled through application of charge-transfer interactions in *rotational* polymorphs, such as tpp, begs the question as to whether the same phenomena can be applied to rigid systems, in which the origin of the polymorphism is due to more subtle packing effects. In order to address this question, we have turned our attention to some simple acridines. Several members of this family have important medicinal uses that include anti-tumor and antibiotic activity.[13] In addition, the parent compound is known to exist in at least five crystalline modifications. Here, we present the results of our investigation into the reaction of iodine with acridine. We find that there is an overwhelming thermodynamic preference for one particular polymorph of this system; this prevents any structural control through intervention of charge-transfer complexes. Iodine complexes of this donor and of 9-chloroacridine do display an unusual structural motif, however, that offers new insights into the synthons accessible with the N···I interaction.

Experimental Section

General: Acridine was obtained from Aldrich Chemical Company and used as received. Resublimed iodine and 9-chloroacridine were purchased from Fisher Scientific. The latter compound was purified by flash chromatography on neutral alumina (eluent: 60:40 petroleum ether/methylene chloride). Solvents were purchased from commercial houses and distilled under argon from appropriate drying agents immediately prior to use.

Thermal gravimetric analysis was performed on a Perkin Elmer Series 7 analyzer. Sample masses ranged from 5 to 10 mg. All samples were heated at a constant rate of 5 °C min^{-1} from 30 °C until all material had vaporized. Elemental analysis was performed on a Perkin Elmer 2400 Series II CHNS analyzer.

Synthesis

*Preparation of acridine$_2\cdot I_6$ (**1**) and 9-chloroacridine$_2\cdot I_6$ (**2**)*: Acridine or 9-chloroacridine (0.50 mmol) was dissolved in methylene chloride and placed in a small vial. Iodine (254 mg, 1.00 mmol) was added, and the solvent was allowed to evaporate until significant quantities of crystalline material had formed. The remaining solvent was removed, and the vial was then sealed until analysis could be conducted. Elemental analysis calcd (%) for $C_{26}H_{18}I_2N_2$ (**1**): C 27.9, H 1.62, N 2.51; found C 32.2, H 1.81, N 2.86; calcd for $C_{26}H_{18}Cl_2I_2N_2$ (**2**): C 26.27, H 1.36, N 2.36; found C 25.29, H 1.31, N 2.16.

Both complexes could also be formed in quantitative yield by exposure of the donor in the solid state to excess I_2 in a sealed vial.

*Preparation of 9-chloroacridine$\cdot I_2$ (**3**)*: This compound was prepared under the same conditions as the solution preparation of **2**, except less I_2 (122 mg, 0.48 mmol) was used.[14]

X-ray diffraction analysis: Single crystal intensity data were measured at 22 ± 1 °C by using $\omega/2\theta$ scans ($2\theta_{max}=50°$) on either a Rigaku AFC7R (18 kW rotating anode generator) diffractometer (**1**) or a Nicolet R3 mV diffractometer (**2** and **3**) with graphite-monochromated $Mo_{K\alpha}$ radiation ($\lambda=0.71073$ Å). The data were corrected for Lorentz and polarization effects. The intensities of three reflections, remeasured periodically throughout data collection, varied by less than 1% for **1** and **3** (this indicated that there was no need for a decay correction). They varied by 10.4% for **2**; a linear correction factor was applied to the data for **2** to account for crystal decomposition. An absorption correction, based on azimuthal (ψ) scans of several intense reflections, was applied to the data for each compound. The structures were solved by direct methods and refined by using full-matrix least-squares techniques. All non-hydrogen atoms were refined anisotropically, and all hydrogen atoms were refined with isotropic displacement parameters for compounds **1** and **3**. Crystal quality of compound **2** was poor; over seven crystals of this compound were studied before a suitable set of data was obtained. Due to the low number of observed data, the phenyl groups were treated as rigid groups ($d_{C-C}=1.395$ Å), but all other non-hydrogen atoms were refined anisotropically. Hydrogen atoms were not included in the model for **2**. Structure solution, refinement, and the calculation of derived results were performed with the *SHELXTL-Plus* package of computer programs.[15] Neutral atom scattering factors and the real and imaginary anomalous dispersion corrections were taken from *International Tables for X-ray Crystallography, Vol. IV*.[16] Relevant crystallographic data are given in Table 1. Crystallographic data

Table 1. Crystal data.

	1	**2**	**3**
formula	$C_{26}H_{18}N_2I_6$	$C_{26}H_{16}N_2Cl_2I_6$	$C_{26}H_{16}N_2Cl_2I_2$
M_w	1119.82	1188.71	681.11
crystal size [mm]	$0.03\times0.08\times0.18$	$0.12\times0.27\times0.34$	$0.24\times0.36\times0.43$
crystal system	triclinic	monoclinic	triclinic
space group	$P\bar{1}$ (No. 2)	$P2_1/n$ (No. 14)	$P\bar{1}$ (No. 2)
a [Å]	9.517(1)	15.018(2)	6.967(4)
b [Å]	11.741(2)	8.770(1)	9.088(3)
c [Å]	7.083(1)	23.525(3)	9.636(2)
α [°]	106.21(2)		83.13(2)
β [°]	92.68(2)	98.30(1)	88.05(4)
γ [°]	106.32(2)		76.11(4)
V [Å^{-3}]	722.6(4)	3066.0(5)	588.0(4)
Z	1	4	1
ρ_{calcd} [g cm^{-3}]	2.57	2.59	1.92
μ [mm^{-1}]	6.47	6.30	2.92
trans. coeff.	0.76/1.00	0.59/1.00	0.74/1.00
no. obsd. data[a]	2130	1491	1875
$R(F_o)$[b]	0.021	0.078	0.027
$R_w(F_o)$[c]	0.026	0.081	0.044

[a] $[I>2\sigma(I)]$. [b] $R=\Sigma\,||F_O|-|F_C||/\Sigma\,|F_O|$. [c] $R_W=[\Sigma w\,|\,|F_O|-|F_C|\,|^2/\Sigma w(F_O)^2]^{1/2}$.

0947-6539/00/0622-4072 $ 17.50+.50/0 *Chem. Eur. J.* **2000**, *6*, No. 22

(excluding structure factors) for the structures reported in this paper have been deposited with the Cambridge Crystallographic Data Centre as supplementary publication nos. CCDC-137946 (**1**), CCDC-137947 (**2**), and CCDC-137948 (**3**). Copies of the data can be obtained free of charge on application to CCDC, 12 Union Road, Cambridge CB2 1EZ, UK (Fax: (+44) 1223-336-033; e-mail: deposit@ccdc.cam.ac.uk).

Powder diffraction data were acquired on a Scintag XDS 2000 theta–theta diffractometer with $Cu_{K\alpha 1}$ radiation ($\lambda = 1.54060$ Å) and an intrinsic germanium solid-state detection system.

Calculations: Density functional theory calculations were carried out using the perturbative Becke–Perdew model as implemented in the Spartan program (version 5.1.1).[17] The DN basis set was used for all geometry optimizations and single point calculations.

Results and Discussion

Selected distances and angles for compounds **1**–**3** are given in Table 2. All figures which include thermal ellipsoid plots have atoms shown at the 50% probability level (except hydrogen atoms, which when shown are set at an arbitrary radius).

Structure of (acridine·I_2)$_2$·I_2: Acridine reacts with iodine both in solution and in the solid state to form an interesting complex (**1**) with the formula, (acridine·I_2)$_2$·I_2. The complex has a complicated structure, in which an iodine molecule complexed to acridine through an $n \rightarrow \sigma^*$ charge-transfer interaction exhibits amphoteric behavior; one end of the I_2 molecule acts as a Lewis acid to the nitrogen donor of the acridine molecule [N(1)···I(1) 2.442(4) Å] and the other end serves as a Lewis base to a second I_2 molecule, also through an $n \rightarrow \sigma^*$ charge-transfer interaction. The I···I interaction [I(3)···I(3a) 3.475(1) Å] is fairly weak and occurs at both ends of the second I_2 molecule to bridge complexes into dimers across an inversion center at the origin (Figure 1). Both charge-transfer interactions result in interatomic contacts, which are considerably shorter than the appropriate van der Waal's radii sums (vdw radius for N is 1.55 Å and for I is 1.98 Å).[18] The N···I interaction is shorter than most of those observed in similar interactions, while the I···I interaction is of the same order as those observed in many polyiodide anions. The (acridine·I_2)$_2$·I_2 dimer has a zigzag conformation with an I(1)–I(2)···I(2a)–I(1a) "torsion angle" of 180°; the iodine atoms of the polyiodine chain are planar (mean deviation is 0.003(4) Å). The dihedral angle between the acridine molecule (planar to 0.02(1) Å) and the iodine plane is 60.7°. Molecular stacking of the acridine rings [interplanar stacking distances of 3.41(2) Å for adjacent rings related by inversion center at (*0 ½ ½*) and 3.36(2) Å for adjacent rings related by inversion center at (*0 ½ 1*)] results in loosely associated layers, which pack to complete the structure (Figure 2).

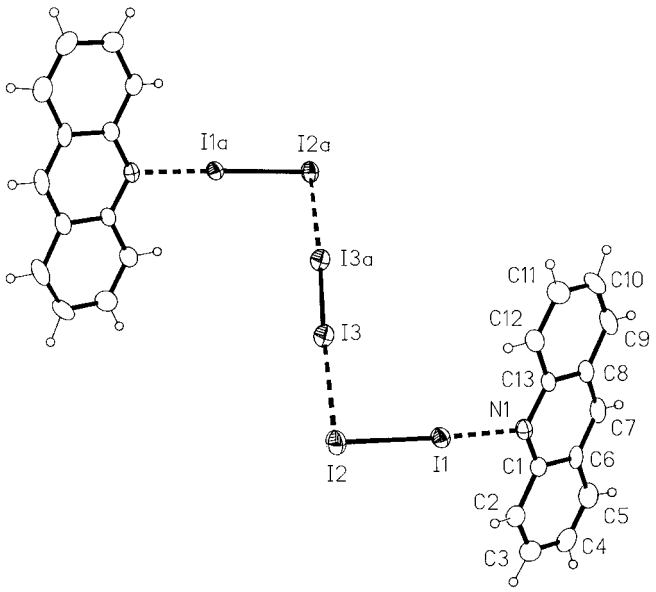

Figure 1. Thermal ellipsoid plot (50% probability) of **1**; this shows the zigzag conformation of the (acridine·I_2)$_2$·I_2 dimer.

Donation of electron density into the σ* orbital of I_2 results in elongation of the I–I bond relative to that observed in elemental I_2 (2.715 Å).[19] This effect is much more pronounced for the N···I interaction [I(1)–I(2) 2.813(1) Å] than for the I···I interaction [I(3)–I(3a) 2.731(1) Å]; this indicates that the former is a considerably stronger interaction. Complexation has little effect on the bonding in the donor, and no significant differences are observed relative to the parent compound.[20]

To the best of our knowledge, **1** is only the second example of

Table 2. Selected bond lengths [Å] and angles [°] for **1**–**3**.[a]

Lengths					
1		**2**		**3**	
I(1)–I(2)	2.813 (1)	I(1)–I(2)	2.750 (4)	I(1)–I(1a)	2.742 (2)
		I(3)–I(4)	2.754 (4)		
I(1)–N(1)	2.442 (4)	I(1)–N(1)	2.62 (3)	I(1)–N(1)	2.980 (3)
		I(3)–N(2)	2.61 (3)		
I(2)–I(3)	3.475 (1)	I(2)–I(5)	3.595 (4)		
		I(4)-I(6)	3.876 (4)		
I(3)–I(3a)	2.731 (1)	I(5)–I(6)	2.720 (7)		
N(1)–C(1)	1.364 (5)	N(1)–C(1)	1.30 (4)	N(1)–C(1)	1.345 (5)
		N(2)–C(14)	1.42 (3)		
N(1)–C(13)	1.368 (6)	N(1)–C(8)	1.37 (4)	N(1)–C(13)	1.353 (4)
		N(2)–C(26)	1.38 (4)		
		Cl(1)–C(7)	1.76 (3)	Cl(1)–C(7)	1.723 (4)
		Cl(2)–C(20)	1.76 (4)		
angles					
1		**2**		**3**	
I(2)–I(1)–N(1)	175.1(1)	I(2)–I(1)–N(1)	177.0(8)	N(1)–I(1)–I(1a)	178.8(1)
		I(4)–I(3)–N(2)	179.3(6)		
I(1)–I(2)–I(3)	80.8(1)	I(1)–I(2)–I(5)	100.9(4)		
		I(3)–I(4)–I(6)	85.5(4)		
I(2)–I(3)–I(3a)	177.2(1)	I(2)–I(5)–I(6)	175.2(4)		
		I(4)–I(6)–I(5)	176.0(4)		

[a] Atoms labeled with a lower-case character were generated by the following symmetry operation: for **1**: a) $-x$, $-y$, $-z$; for **3**: a) $1-x$, $1-y$, $1-z$.

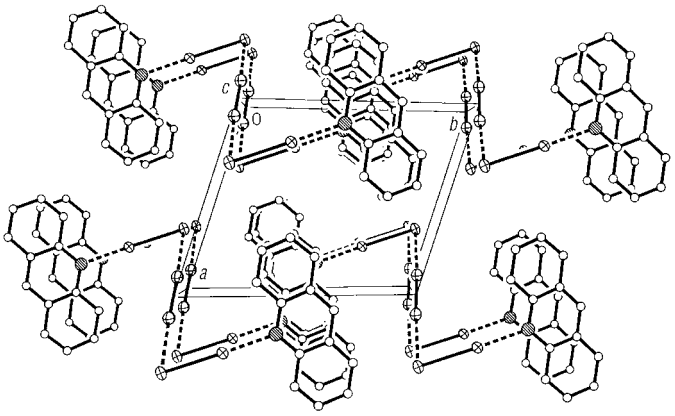

Figure 2. Crystal packing of **1**, viewed down the *c*-axis ($+x$ is down, $+y$ is to the right).

an N···I charge-transfer complex that involves an amphoteric I_2 molecule, although similar complexes that involve sulfur[21] and selenium[22] have been observed. In the only other example, (2,2′-bipyridine·$2I_2$)·I_2,[23] the I_6 chain has a similar zigzag conformation, but the N···I interaction is considerably weaker [2.60(3) Å] as is the I···I interaction [3.550(6) Å]. It is interesting to note that this complex is stabilized by extended interactions, as the interactions link the molecules into an infinite chain.

Previously, we have noted that most N···I charge-transfer complexes fall into two categories.[9b] Complexes with weak donors possess N···I interactions at either end of the I_2 molecule, but they can only be isolated when two or more donor sites are available (e.g. diazinyl donors such as pyrazine and derivatives) to lead to extended interactions, which stabilize the complex structure. Stronger donors, such as pyridine derivatives, typically give simple molecular adducts with N···I interaction that occurs at only one end of the I_2 molecule. This is presumably due to polarization of the I_2 molecule and results in an increase in the partial charge on the terminal iodine atom. Acridine is a stronger base ($pK_a = 5.60$)[24] than most of the donor molecules, which lead to molecular adducts. In order to determine whether the unusual structure of **1** is due to its increased basicity, we have investigated acridine derivatives with either an electron-donating (methyl) or electron-withdrawing (chloro) substituent in the 9-position. Study of the former was complicated by iodination of the methyl group,[9a] but the latter formed a dimeric complex (**2**) that contains a similar I_6 chain with amphoteric I_2s bridged by I_2 and capped by the neutral donor molecules; this has a significantly different conformation and packing.

Structure of (9-Cl-acrid·I_2)$_2$·I_2: In spite of its reduced donor ability, 9-chloroacridine reacts with excess iodine to form a complex with the formula, (9-Cl-acrid·I_2)$_2$·I_2, which has similar connectivity to **1**. Unlike **1**, the entire formula unit occupies a general position within the unit cell. The electron-withdrawing effect of the chloro substituent reduces the donating ability of the nitrogen atom, and this leads to considerably longer N···I contacts [N(1)–I(1) 2.62(3) Å and N(2)–I(3) 2.61(3) Å]. The reduced strength of the interaction also leads to weaker I···I interactions at the other end of the I_2 molecule [I(2)···I(5) 3.595(4) Å and I(4)···I(6) 3.876(4) Å] and to less elongation of the I_2 bonds [I(1)–I(2) 2.750(4) Å, I(3)–I(4) 2.754(4) Å, and I(5)–I(6) 2.720(7) Å].

As in **1**, the I_6 chain is essentially planar (mean deviation of 0.07(4) Å), but rather than a zigzag conformation, the chain is C-shaped (Figure 3); the I(1)–I(2)···I(4)–I(3) "torsion angle" is 3.1°. The dihedral angles between the acridine ring

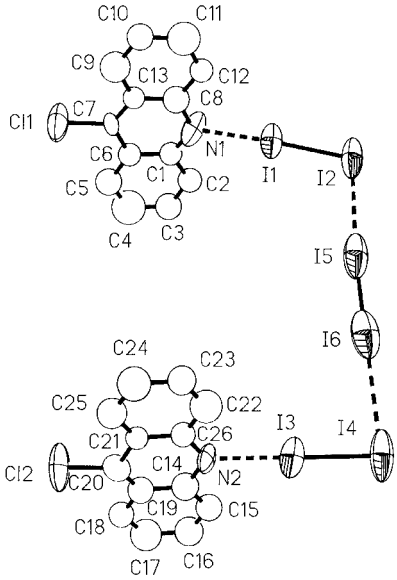

Figure 3. Thermal ellipsoid plot (50% probability) of **2**; this shows the C-shaped conformation of the (9-Cl-acridine·I_2)$_2$·I_2 dimer.

planes and the plane through the iodine atoms are 69.1° for the ring containing N(1) and 68.5° for the ring containing N(2), respectively. The dimers stack in an interlocking fashion (Figure 4) to form columns, which pack to complete the crystal. The interplanar stacking distances range from 3.45(3) to 3.51(2) Å.

The structures of both **1** and **2** bear a striking resemblance to polyiodide anions and can be thought of as donor-capped neutral polyiodine chains based on I_8^{2-} (in an $I_3^- \cdot I_2 \cdot I_3^-$ configuration). In particular, the structure of **1** closely resembles the zigzag I_8^{2-} anion found in bis(methyltriphenylphosphonium)octaiodide[25] and in platinum and palladium coordinated macrocyclic salts of I_8^{2-} (although the anion is nonplanar in this system).[26] The structure of **2** is analogous to a C-shaped I_8^{2-} anionic structure, which is composed of half of an I_{16}^{4-} anion in (theobromine)$_2$·H_2I_8.[27] Recently, Hoffman and coworkers have reported a systematic investigation of the bonding in trihalides, mixed trihalides, and hydrogen bihalides[28] using a donor–acceptor approach to establish connections between hypervalent bonding, electron-rich three-center bonding, strong hydrogen bonding, and donor–acceptor interactions. They suggest that a pseudolinear QXX unit (Q = donor, X = halogen), such as is observed in **1** and **2**, can be well understood in terms of an electronegativity perturbation of a X_3^- anion. As is discussed below, a similar conceptual approach is useful for understanding these systems.

Acridine polymorphs and the decomposition of 1: Five crystalline modifications of acridine have been reported in the literature, and these include a metastable hydrate

0947-6539/00/0622-4074 $ 17.50+.50/0 *Chem. Eur. J.* **2000**, *6*, No. 22

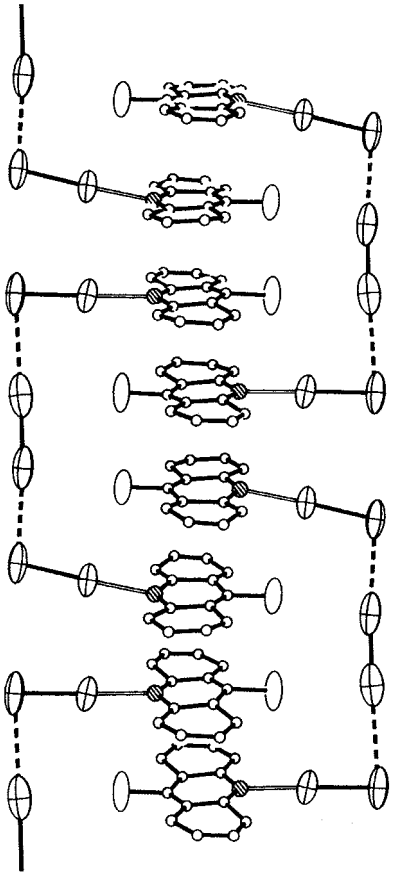

Figure 4. Stack of interlocking dimers of **2**.

(form **I**).[29] Of these, form **II** is probably the most thermodynamically stable form,[15a] as forms **I**, **III**, and **IV** can all be converted to **II** at elevated temperature (form **V** is also not thermally stable, but its decomposition is not well described). Interestingly, the density of **II** is lower than that of **III** (1.283 g mol^{-1} vs. 1.296 g mol^{-1}), and **II** crystallizes with two unique molecules/asymmetric unit, while **III** contains only one molecule/asymmetric unit. These two observations indicate that **II** is less efficiently packed than **III**, but may be favored due to entropic terms.[30]

Close inspection of the structures of polymorphs **II** and **III** reveals that both contain C–H···N bridged dimers (Figure 5),[31] but the interaction is considerably stronger in **II** than in **III** (H···N length of 2.59 Å in **II**[29d] versus 2.84 Å in **III**[29c]).

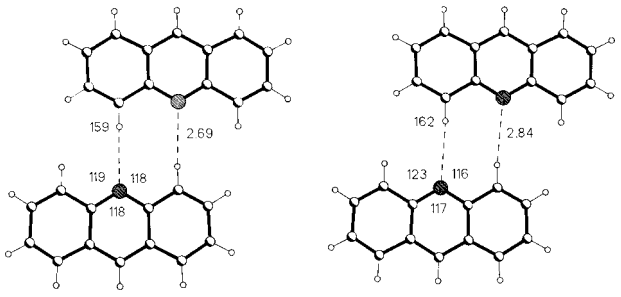

Figure 5. C–H···N linked dimers in acridine polymorphs a) form II and b) form III.

In both polymorphs, deeply tilted stacks of these dimers form columns along the shortest crystallographic axis; additional acridine molecules fill "stair-step" gaps in the columns in a "herringbone" fashion. In **II**, these interactions involve a second unique set of acridine molecules, which do not take part in any C–H···N interactions, while in **III** they are accomplished by acridine molecules of adjacent columns on either side. Due to differences in the interactions between the columns, the shape of the columnar structures, which consist of the deeply tilted stack of C–H···N bridged dimers with additional acridine molecules to fill the gaps, is different for the two forms. In **II**, the molecules which interact with the column are shifted toward the C–H···N bonded side of the dimer to give an "S-shaped" column (Figure 6a), while in **III**,

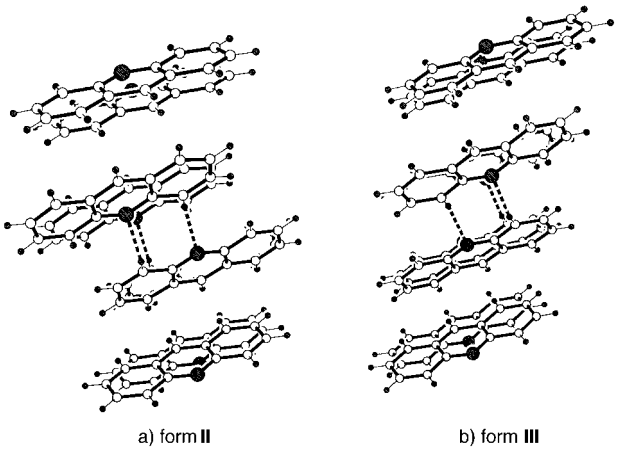

Figure 6. a) S-shaped and b) rhomboidal columns of stacked dimers in acridine polymorphs a) form II and b) form III.

the molecules which interact with the column (which are part of adjacent columns) shift toward the opposite side of the dimer to give smoother rhomboidal columns (Figure 6b). Presumably, the supramolecular conformation of the columnar structure in **II** is energetically more favorable than that in **III**, as evidenced by its stronger C–H···N hydrogen bonding, but the conformation in **III** has better packing efficiency due to the ability of adjacent columns to mesh together (Figure 7), as confirmed by its greater density. If form **III** (and presumably **I** and **IV**) is heated, this allows the formation of the more stable "supramolecule", which then crystallizes as form **II**.

Decomposition of **1** through diffusion of I_2 occurs over the span of several weeks (or more quickly with heating or reduced pressure) and gives polymorph **II** as the sole product (as verified by powder diffraction). Similarities between the structure of the complex, **1**, and its product, form **II**, are not as conclusive for the explanation of the decomposition mechanism as for the tpp system.[9c,10] A more plausible explanation seems to be that upon loss of I_2 (which unlike that in the tpp complexes, comprises a major component of the packing volume) the packing of the acridine molecules is so disrupted that an environment similar to that of heating occurs; this allows the formation of the most stable column conformation and subsequent crystallization as the form **II** polymorph.

Thermal behavior of 1 and 2: While compound **1** loses I_2 at room temperature, complete removal of halogen is a complex process and can only be achieved at elevated temperatures. Figure 8 shows the change in mass of bulk samples of **1** and **2** as the temperature was increased from ambient at a rate of $5\,^{\circ}C\,min^{-1}$. Curves A, B, and C are standards of acridine, 9-chloroacridine, and iodine, respectively. Curves D and E are representative samples of **1** and **2**, respectively. These data are quantified in Table 3, in which the onset and mass change of each thermal event is listed along with a proposed explanation of the change.

Compound **1** only slowly lost I_2 at ambient temperature. At 58 °C, there was a slight acceleration, but the initial mass loss is a very poorly defined event. At approximately 110 °C, one equivalent of I_2 evolved from the complex. A second, somewhat better defined event began with an onset temperature of 136 °C. The mass loss at this stage corresponds to the remaining I_2. The final major thermal event, with an onset of 179 °C, was the sublimation of acridine. A small quantity of material remained above 250 °C, and this was likely to be due to the formation of an acridine salt, formed by I_2 oxidation. This reaction is often observed during the thermolysis of I_2 charge-transfer complexes.

The diffusion of the first equivalent of I_2 from the surface of the sample results in a contraction of the lattice. This in turn makes it more difficult for I_2 in the interior of the crystals to escape and explains the broad, ill-defined mass loss observed. This may also be an indication of an intermediate complex in the thermolysis process, which has a 1:1 acridine/I_2 ratio. If present, this intermediate is only marginally stable, as evidenced by the lack of a plateau in the data. The room-temperature loss of I_2 to give the form **II** polymorph of acridine can be easily monitored by x-ray powder diffraction (Figure 9).

Thermal gravimetric analysis of complex **2** (Figure 8, curve E) also showed multiple mass losses prior to sublimation of the organic moiety. Again, there was an ill-defined loss of I_2 that began at ambient temperature. This quickly leveled off as the surface of the crystals reorganized to a more compact form. A sharp mass loss with an onset temperature of 87 °C resulted in the complete disruption of the matrix and loss of two full equivalents of I_2. A significant plateau was observed around 125 °C; this

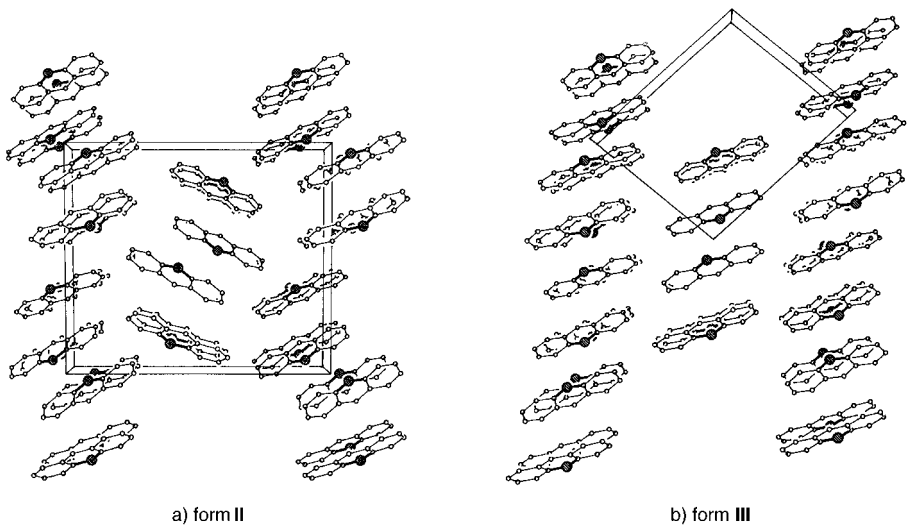

Figure 7. Crystal packing of columns in acridine polymorphs a) form II and b) form III.

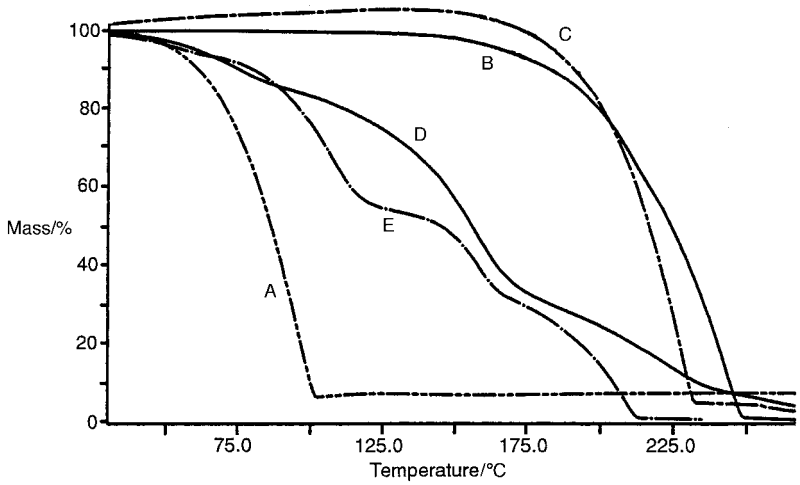

Figure 8. Thermal gravimetric analysis data for: A) iodine, B) 9-Cl-acridine, C) acridine, D) compound **1**, and E) compound **2**.

Table 3. Thermal gravimetric analysis data for **1** and **2**.

	Onset Temp. [°C]	Mass Loss [wt.%][a]	Description
iodine	57	≈100[a]	evaporation
acridine	179	≈100[a]	evaporation
9-Cl-acridine	190	≈100[a]	evaporation
1	58	14	**1**⟶acridine · I_2
	136	55	acridine · I_2⟶acridine
	179	27[a]	evaporation
2	87	45	**2**⟶[Cl-acridine]$_2$ · I_2
	146	24	[Cl-acridine]$_2$ · I_2⟶Cl-acridine
	194	29[a]	evaporation

[a] Small residual mass due to instrument drift or side reactions.

0947-6539/00/0622-4076 $ 17.50+.50/0 *Chem. Eur. J.* **2000**, *6*, No. 22

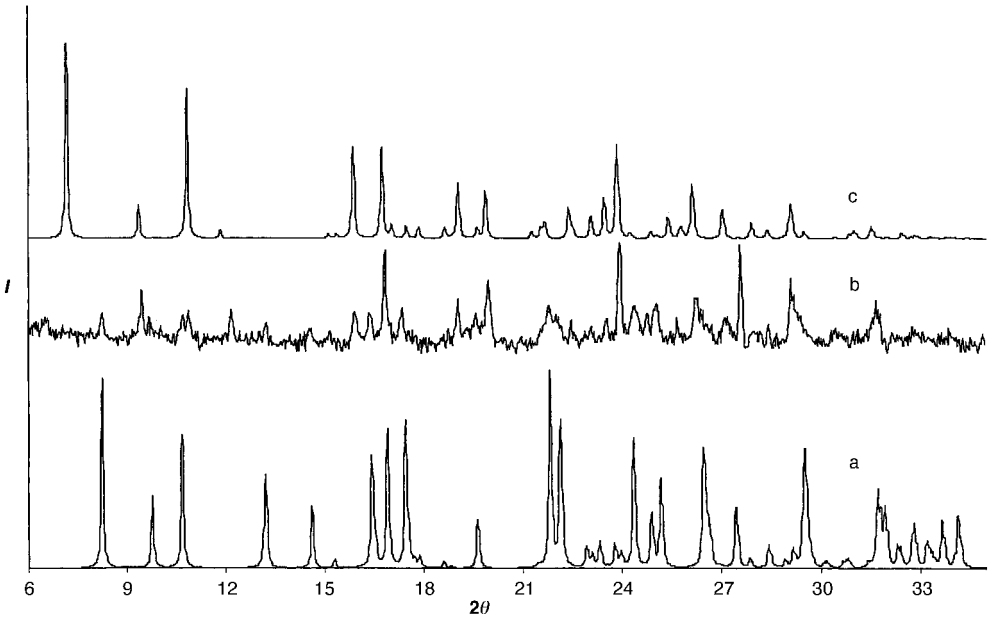

Figure 9. Powder x-ray diffraction data for decomposition of **1**: a) calculated pattern for **1**, b) partially decomposed sample of **1** (approximately one week at 25 °C), and c) calculated pattern for acridine (polymorph II).

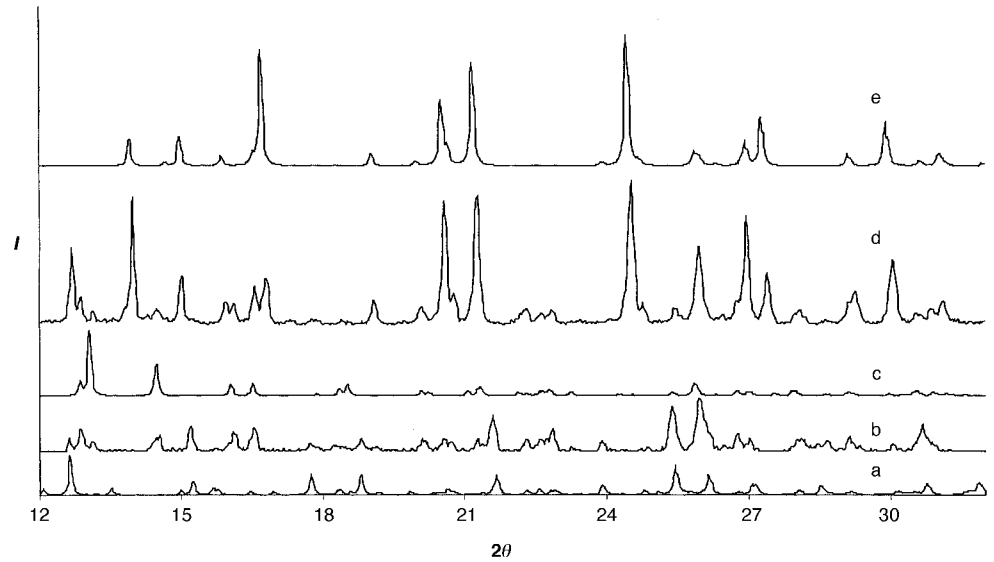

Figure 10. Powder x-ray diffraction data for decomposition of **2**: a) calculated pattern for **2**, b) sample after decomposition for approximately three hours at 25 °C, and c) calculated pattern for **3**, d) sample after decomposition for approximately eighteen hours at 25 °C, and e) calculated pattern for 9-Cl-acridine.

suggests that a reasonably stable intermediate (complex **3**) with a 9-chloroacridine/I_2 ratio of 2:1 was formed. At higher temperature, the remaining I_2 evolved, followed by the chloroacridine.

As with the decomposition of **1**, powder x-ray diffraction revealed that both the room-temperature loss of I_2 and heating the product to 125 °C lead to a decrease in the amount of **2** and the formation of the same, microcrystalline product (Figure 10). In this case, however, the greater stability of this intermediate allowed single crystals to be grown from I_2-deficient solutions. As was anticipated from the thermochemistry, **3** does have a 2:1 9-chloroacridine/I_2 ratio.

Structure of (9-Cl-acrid)$_2$·I$_2$: Contrary to our previous observation that complexes with interactions at either end of an I_2 molecule are only isolated in extended structures with weak donor molecules with multiple sites, this complex forms as a simple 2:1 adduct, in which two donor molecules are bridged by an I_2 molecule (Figure 11). The N···I distance in **3** is considerably longer [2.980(3) Å] than in the amphoteric complex, **2** [2.61(3)–2.62(3) Å]; this is consistent with the expected reduction in acceptor strength with two donor–acceptor interactions. The N···I–I interactions are linear [177.0(8) and 179.3(6)°], as expected. The acridine ring is planar [mean deviation, 0.014(9) Å]; the chlorine atom is within the plane [−0.035 Å], while the iodine atom is significantly out of the plane [0.790 Å]. The 2:1 adducts of **3** stack along the *a*-axis with a mean interplanar spacing of 3.46(2) Å. There are no significantly close intermolecular contacts between adducts.

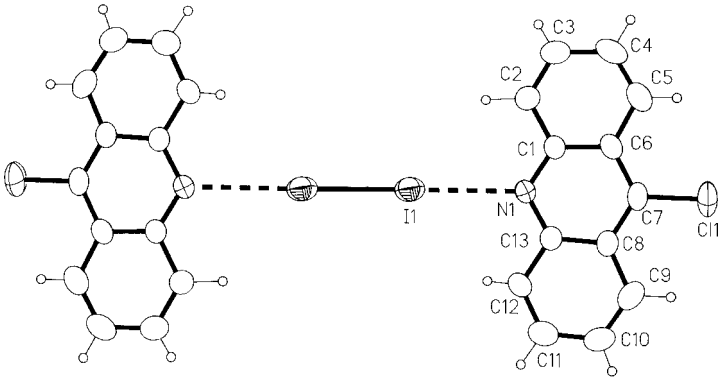

Figure 11. Thermal ellipsoid plot (50% probability) of **3**.

A computer simulation of iodine in pyridine has predicted that pyridine and iodine molecules would associate to form long-lasting (2:1) complexes, which would adopt a nearly linear py–I_2–py conformation,[32] like that of **3**. However, to the best of our knowledge, **3** represents the first observed example of this type of complex in the solid state.

Quantum mechanical interpretation of the bonding in N···I charge-transfer complexes: The bonding in compounds **1–3** can best be understood through an examination of the molecular orbitals involved. We[33] and others[34] have found that Hartree–Fock (HF) methods do not give satisfactory geometries for iodine charge-transfer complexes, as they grossly overestimate the N–I bond length. Conversely, density functional theory (DFT) works quite well, even with a minimal basis set. The N···I bond length is still typically overestimated by 0.1–0.3 Å, but this will be sufficient for the qualitative analysis presented below. From a MO viewpoint, the acridine and 9-chloroacridine systems are very similar. We will, therefore, focus this discussion on the 9-chloroacridine complexes and comment briefly on the differences between the two donors.

It is convenient to build up to the bonding in **2** and **3** by first discussing the hypothetical 1:1 CT complex, **4**. While this particular species has not been observed, there is ample precedence for this structure with other nitrogen heterocycles, and it is possible that it is the first complex formed in solution. The charge-transfer interaction is generally accepted to result from the interaction of the nitrogen lone pair on the donor (Φ_D) and the σ-bonding (σ_A) and antibonding (σ_A^*) orbitals on the I_2. The latter are formed primarily from p orbitals on the iodines (with some s contribution). Figure 12 shows a fragment molecular orbital interaction diagram for the Rundle–Pimentel three-orbital/four-electron model.[35] In the case of **4**, Φ_D is slightly higher in energy than is σ_A^*.

The composite orbitals, 1σ, 2σ, and 3σ are the HOMO-10, the HOMO-5, and the LUMO orbitals, respectively, and are shown in Figure 13. The remaining orbitals near the frontier that are not shown are various π-type orbitals (such as the HOMO), which do not play a significant role in the N···I bonding interaction, since the orbitals of π-symmetry in the acceptor are completely full. The primary source of bonding is 1σ. This orbital mostly consists of contributions from Φ_D and

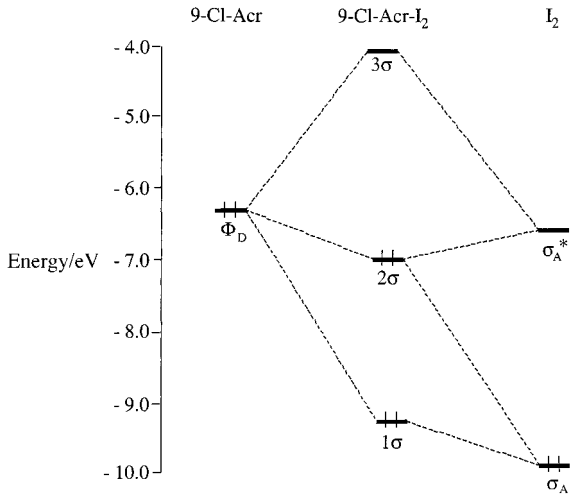

Figure 12. Fragment molecular orbital interaction diagram for **4**. All of the orbitals shown have σ symmetry.

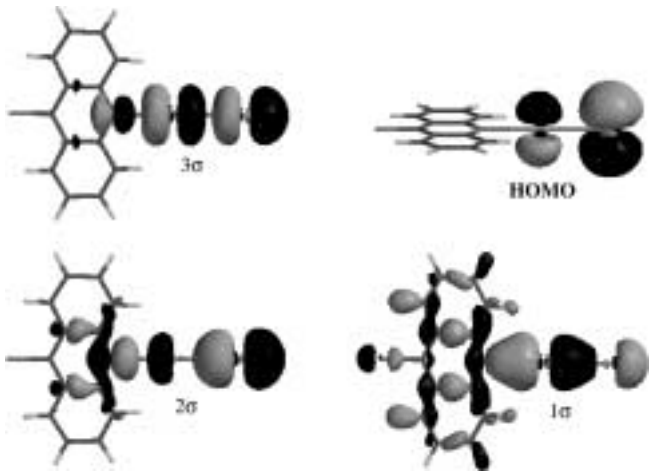

Figure 13. The frontier σ MOs and the HOMO of **4**.

σ_A. The next orbital, 2σ, is shown with a small bonding interaction between the iodines and antibonding at N···I (there are also very small bonding interactions within the aromatic ring σ-system). The mixing of σ_A and σ_A^* decreases the contribution of the p atomic orbital on the central iodine and increases the importance of the s character; the phase of this determines the nature of the interaction between the three atoms under discussion. Thus, 2σ is very sensitive to donor strength. As the strength of the donor increases, 2σ becomes more bonding between the donor and acceptor and more antibonding between the iodine atoms.[34] Since we know that our calculation overestimates the N···I bond length, the description of 2σ in Figure 13 must be recognized as somewhat exaggerated. The parent acridine is a better donor yet and gives a stronger N···I interaction and weakens the I–I bond relative to **4**. Thus, while the orbital picture presented here is qualitatively correct, experimentally there is a greater net transfer of electrons to the iodines as well as a greater elongation of the I–I bond due to the increased antibonding character between these atoms in 2σ.

Starting from **4**, we can construct fragment molecular orbital interaction diagrams for **2** and **3** by the addition of the

  0947-6539/00/0622-4078 $ 17.50+.50/0 *Chem. Eur. J.* **2000**, *6*, No. 22

appropriate components. Interestingly, **2** requires that the terminal iodine acts as an electron donor, while **3** requires that the very same atom acts as an electron acceptor. Formation of the latter complex is especially counterintuitive since the charge-transfer interaction in **4** leads to a net transfer of electrons onto the I_2 moiety, particularly the terminal iodine. Clearly, the formation of a second N···I bond is made more difficult by the increase in electrostatic repulsion between the terminal iodine and the second nitrogen lone pair. Yet the orbitals on iodine are quite diffuse, and provided there is not too much charge buildup on the terminal iodine, the attraction between the iodine electron cloud and the nitrogen nucleus is significant.[28]

Figure 14 shows the fragment molecular orbital interaction diagram for the formation of bis(9-chloroacridine)·I_2, **5**, at its calculated gas-phase minimum energy geometry. This differs

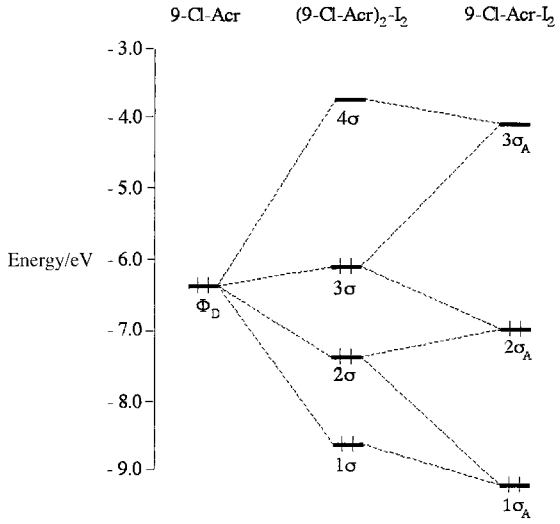

Figure 14. Fragment molecular orbital interaction diagram for **5**. All of the orbitals shown have σ symmetry.

from the geometry of the solid-state structure, **3**, in some important respects (see below). The diagram considers **5** to be formed from **4** and 9-chloroacridine; the orbitals 1σ, 2σ, and 3σ from Figure 12 are now labeled $1\sigma_A$, $2\sigma_A$, and $3\sigma_A$, respectively. Figure 15 shows a representation of the four critical orbitals in **5**, 1σ–4σ, that correspond to HOMO-16, HOMO-8, HOMO-2, and LUMO + 2, respectively. Again,

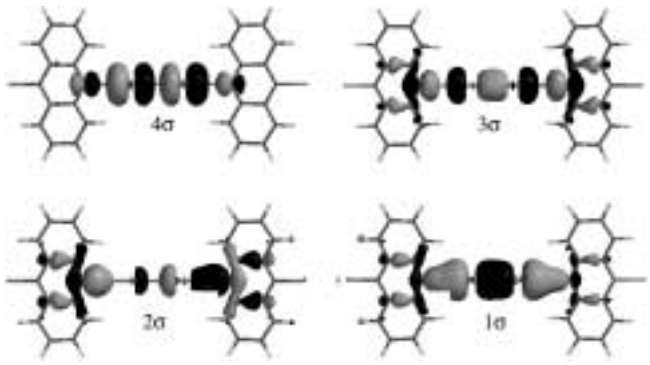

Figure 15. The frontier σ MOs of **5**.

the remaining orbitals in this energy regime are composed of π-type orbitals that play no significant role in the charge-transfer interaction, since the iodine p orbitals are completely filled. The orbitals in Figure 15 are similar to those shown in Figure 13. The primary bonding orbital is 1σ, while the unoccupied orbital 4σ is antibonding between the four participating atoms. The orbital 2σ is N···I bonding and I–I antibonding, while 3σ is the reverse. In each of the three occupied orbitals, there are also minor contributions from carbon-based orbitals.

The calculated N···I bond length in **5** is 2.876 Å, or 0.1 Å shorter than that observed in the solid-state complex **3**. The I–I bond length is calculated to be 3.036 Å vs. the observed value of 2.742 Å. Unlike DFT calculations on other charge-transfer complexes, the extent of electron donation to the iodine is overestimated significantly. This is because packing requirements in the solid force the N···I–I bond angle to deviate from linearity by about 3°. As was observed by Hoffmann in his study of trihalide anions,[28] this distortion causes a large decrease in the orbital interaction energy term between the donor and acceptor. Another consequence of this bending is that it results in the mixing of the π-system into the σ-framework. While the general orbital scheme shown in Figures 14 and 15 remains the same, it is complicated by the inclusion of partial σ character in additional orbitals.

The bonding in complex **2** can be viewed as simply a combination of that in **4** and in **5**. The central iodine acts as an electron acceptor at both ends, as in **5**, while the donor is the HOMO of the 1:1 adduct, **4**. The donor orbital is the π-antibonding orbital that results from the destructive overlap of the I_2 lone pairs perpendicular to the plane of the heterocycle (Figure 13). The donor HOMO-1 is very similar to the HOMO in both energy and shape. It lies parallel to the molecular plane, however, so steric interactions prevent the use of this orbital for bonding. The two donors interact with the I_2 σ and σ* orbitals and give a four orbital, six electron system analogous to that in Figure 14. As with compound **3**, the actual orbital picture for **2** is quite intricate due to solid-state packing requirements that twist the complex from its minimum-energy molecular geometry. This results in considerable mixing of the σ- and π-systems. Structure **6** maintains the N···I and I–I lengths observed in **2**, but the bond angles have been artificially adjusted to minimize (though not completely eliminate) this orbital mixing. Figure 16 shows representations of the four orbitals involved in the bonding of the central I_2 moiety. It is clear that the donor/acceptor interaction is very weak; σ_1 and σ_4 (the HOMO-26 and LUMO + 4, respectively) are primarily the I_2 σ and σ* orbitals. Likewise, σ_2 (HOMO-5) and σ_3 (HOMO-2) are localized mainly on the donor fragments.

Conclusion

Like 2,2′-bipyridine, acridine and 9-chloroacridine form unusual charge-transfer complexes with iodine, in which an I_2 molecule exhibits amphoteric behavior. The overlap in donor strengths of these nitrogen heterocycles relative to those involved in molecular adducts suggests that their

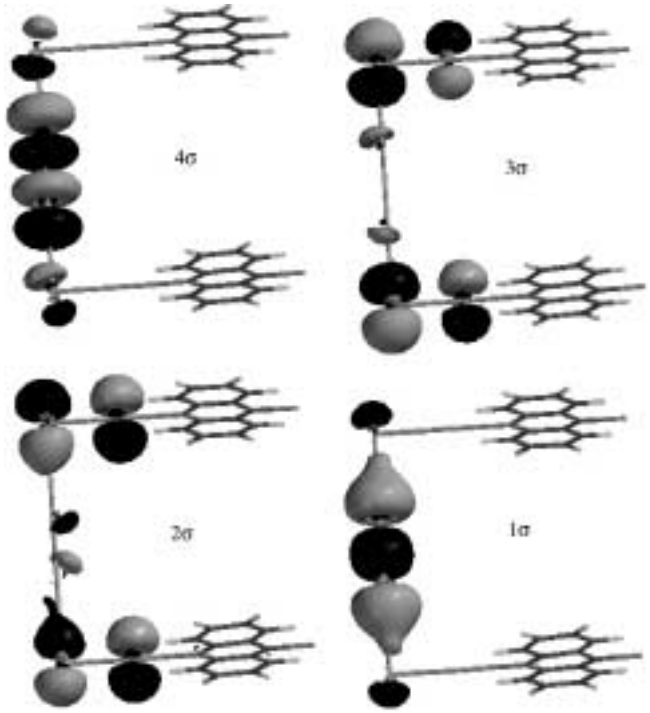

Figure 16. The frontier σ MOs of **6**.

formation is due more to the size and shape of the donor than to electronic factors related to donor strength and the resulting perturbation of the I_2 molecule. The neutral polyiodine chains of **1** and **2** bear striking resemblance to polyiodide anions and can be viewed as intermediates to ionic species. As with polyiodides, this class of compounds is expected to exhibit great structural diversity as a function of the neutral donor capping molecules. Both acridine and 9-chloroacridine exhibit interesting iodine sponge behavior, in which iodine can be inserted and removed through relatively facile solid-state processes. Further investigations into this interesting class of complexes will explore their structural diversity as well as their unusual thermal behavior.

Acknowledgements

Support of this work by Research Corp., the Petroleum Research Fund, and the National Science Foundation (for purchase of the rotating anode x-ray system used in this study) is gratefully acknowledged.

[1] For recent examples, see: a) S. C. Zimmerman, *Science* **1997**, *276*, 543; b) V. A. Russell, M. D. Ward, *Chem. Mater.* **1996**, *8*, 1654; c) D. Braga, F. Grepioni, *Chem. Commun.* **1996**, 571; d) M. J. Zaworotko in *Electrical and Optical Polymer Systems*: *Fundamental*, *Methods and Applications* (Eds.: D. L. Wise, G. E. Wnek, D. J. Trantolo, T. M. Cooper, J. D. Gresser), Marcel Dekker, New York, **1998**, Chapter 25; e) R. Bishop, *Chem. Soc. Rev.* **1996**, *25*, 311; f) P. J. Langley, J. Hullinger, *Chem. Soc. Rev.* **1999**, *5*, 279.

[2] E. J. Corey, *Pure Appl. Chem.* **1967**, *14*, 19.

[3] a) G. R. Desiraju, *Angew. Chem.* **1995**, *107*, 2541; *Angew. Chem. Int. Ed. Engl.* **1995**, *34*, 2311; b) V. R. Thalladi, B. S. Goud, V. J. Hoy, F. H. Allen, J. A. K. Howard, G. R. Desiraju, *Chem. Commun.* **1996**, 401; c) G. R. Desiraju, *Chem. Commun.* **1997**, 1475.

[4] For recent examples, see: a) J. Perlstein, K. Steppe, S. Vaday, E. M. N. Ndip, *J. Am. Chem. Soc.* **1996**, *118*, 8433; b) P. Brunet, M. Simard, J. D. Wuest, *J. Am. Chem. Soc.* **1997**, *119*, 2737; c) D. Endo, T. Ezuhara, M. Koyanagi, H. Masuda, Y. Aoyama, *J. Am. Chem. Soc.* **1997**, *119*, 499; d) O. M. Yaghi, H. Li, T. L. Groy, *J. Am. Chem. Soc.* **1996**, *118*, 9096; e) C. B. Aakeroy, A. M. Beatty, *Crystal Eng.* **1998**, *1*, 39.

[5] This is the estimated energy of a C–Cl···N interaction from calculations performed on a dimer of chlorocyanoacetylene: J. P. M. Lommerse, A. J. Stone, R. Taylor, F. H. Allen, *J. Am. Chem. Soc.* **1996**, *118*, 3108. The strength of this C–X···N interaction increases from chlorine to bromine to iodine, and would be expected to be stronger still for the dihalides.

[6] R. S. Mulliken, *J. Am. Chem. Soc.* **1952**, *74*, 811.

[7] a) R. Foster, *Organic Charge-Transfer Complexes*, Academic Press, New York, **1969**; b) C. K. Prout, J. D. Wright, *Angew. Chem.* **1968**, *80*, 688; *Angew. Chem. Int. Ed. Engl.* **1968**, *7*, 659; c) H. A. Bent, *Chem. Rev.* **1968**, 587.

[8] a) H. M. Yamamoto, J.-I. Yamaura, R. Kato, *J. Am. Chem. Soc.* **1998**, *120*, 5905; b) R. Weiss, M. Rechinger, F. Hampel, A. Wolski, *Angew. Chem.* **1995**, *107*, 483; *Angew. Chem. Int. Ed. Engl.* **1995**, *34*, 441; c) V. Amico, S. V. Meille, E. Corradi, M. T. Messina, G. Resnati, *J. Am. Chem. Soc.* **1998**, *120*, 8261; d) T. Imakubo, T. Maruyama, H. Sawa, K. Kobayashi, *Chem. Commun.* **1998**, 2021; e) J. Grebe, G. Geiseler, K. Harms, B. Neumuller, K. Dehnicke, *Angew. Chem.* **1999**, *111*, 183; *Angew. Chem. Int. Ed.* **1999**, *38*, 222; f) D. S. Reddy, D. C. Craig, A. D. Rae, G. R. Desiraju, *J. Chem. Soc. Chem. Commun.* **1993**, 1737; g) A. A.-A. A. Boraei, E. M. A. Alla, M. R. Mahmoud, *Chem. Soc. Jpn.* **1994**, *67*, 603; h) S. Aronson, S. B. Wilensky, T.-I. Yeh, D. Degraff, G. M. Wieder, *Can. J. Chem.* **1986**, *64*, 2060; i) H. S. Randhava, L. S. Sandhu, *Z. Phys. Chem. Leipzig* **1986**, *267*, 168; j) P. C. Dwivedi, A. K. Banga, *J. Inorg. Nucl. Chem.* **1980**, *42*, 1767; k) V. G. Krishna, B. B. Bhowmik, *J. Am. Chem. Soc.* **1968**, *90*, 1700; l) V. G. Krishna, M. Chowdhury, *J. Phys. Chem.* **1963**, *67*, 1067; m) J. N. Chaudhuri, S. Basu, *Trans. Faraday Soc.* **1959**, *55*, 898.

[9] a) E. L. Rimmer, R. D. Bailey, W. T. Pennington, T. W. Hanks, *J. Chem. Soc. Perkin Trans. 2* **1998**, 2557; b) R. D. Bailey, G. W. Drake, M. Grabarczyk, T. W. Hanks, L. L. Hook, W. T. Pennington, *J. Chem. Soc. Perkin Trans. 2* **1997**, 2773; c) R. D. Bailey, M. Grabarczyk, T. W. Hanks, W. T. Pennington, *J. Chem. Soc. Perkin Trans. 2* **1997**, 2781; d) R. D. Bailey, M. L. Buchanan, W. T. Pennington, *Acta Crystallogr. Sect. C* **1992**, *C48*, 2259; e) R. D. Bailey, L. L. Hook, R. P. Watson, T. W. Hanks, W. T. Pennington, *Cryst. Eng.* **2000**, in press.

[10] R. D. Bailey, M. Grabarczyk, T. W. Hanks, E. M. Newton, W. T. Pennington, *Electronic Conference on Trends in Organic Chemistry* (*ECTOC-1*) (Eds.: H. S. Rzepa, J. M. Goodman (CD-ROM)), Royal Society of Chemistry, **1995**. See also http://www.ch.ic.ac.uk/ectoc/papers.

[11] a) P. S. Skell, R. R. Pavlis, D. C. Lewis, K. S. Shea, *J. Am. Chem. Soc.* **1973**, *95*, 6735; b) S. H. Wilen, K. A. Bunding, C. M. Kascheres, M. J. Weider, *J. Am. Chem. Soc.* **1985**, *107*, 6997; c) A. Farina, S. V. Meille, M. T. Messina, P. Metrangolo, G. Resnati, G. Vecchio, *Angew. Chem.* **1999**, *111*, 2585; *Angew. Chem. Int. Ed.* **1999**, *38*, 2433.

[12] D. Phelps, A. Crihfield, J. Hartwell, T. W. Hanks, W. R. Pennington, R. D. Bailey, *Mol. Cryst. Liq. Cryst. Sci. Technol. Sect. A* **2000**, in press.

[13] a) Y.-P. Pang, P. Quiram, T. Jelacic, F. Hong, S. Brimijoin, *J. Biol. Chem.* **1996**, *271*, 23646; b) T. D. Sakore, B. S. Reddy, H. M. Sobell, *J. Mol. Biol.* **1979**, *135*, 763; c) B. E. Bowler, S. J. Lippard, *Biochemistry* **1986**, *25*, 3031.

[14] Elemental analysis was not performed on this sample, because a significant amount of starting hydrocarbon co-precipitated with the product.

[15] G. M. Sheldrick, *SHELXTL*, *Crystallographic Computing System*, Nicolet Instruments Division: Madison, WI, **1986**.

[16] *International Tables for X-ray Crystallography Vol. IV.* Kynoch, Birmingham, **1974**.

[17] *SPARTAN*, *Version 5.1.1*: Wavefunction, 18401 Von Karman Avenue, Suite 370, Irvine, CA 92612.

[18] A. Bondi, *J. Phys. Chem.* **1964**, *68*, 441.

[19] F. van Bolius, P. B. Koster, T. Migchelsen, *Acta Crystallogr.* **1967**, *23*, 90.

[20] a) A. I. Kitaigorodskii, *Molecular Crystals and Molecules*, Academic Press, New York, **1973**; b) R. D. Lowde, D. C. Phillips, R. G. Wood, *Acta Crystallogr.* **1953**, *6*, 553; c) D. C. Phillips, *Acta Crystallogr.* **1956**, *9* , 237; d) D. C. Phillips, F. R. Ahmed, W. H. Barnes, *Acta Crystallogr.*

  0947-6539/00/0622-4080 $ 17.50+.50/0

1960, *13*, 365; e) B. P. Clarke, J. M. Thomas, J. O. Williams, *Chem. Phys. Lett.* **1975**, *35*, 251; f) F. H. Herbstein, G. M. J. Schmidt, *Acta Crystallogr.* **1955**, *8*, 399.
[21] a) W. W. Schweikert, E. A. Meyers, *J. Phys. Chem.* **1968**, *72*, 1561; b) F. H. Herbstein, W. Schwotzer, *Angew. Chem.* **1982**, *94*, 222; *Angew. Chem. Int. Ed. Engl.* **1982**, *21*, 219; c) F. H. Herbstein, W. Schwotzer, *J. Am. Chem. Soc.* **1984**, *106*, 2367.
[22] F. Cristiani, F. Demartin, F. A. Devillanova, F. Isaia, V. Lippolis, G. Verani, *Inorg. Chem.* **1994**, *33*, 6315.
[23] S. Pohl, *Z. Naturforsch. B* **1983**, *B38*, 1535.
[24] A. Albert, R. Goldacre, J. Phillips, *J. Chem. Soc.* **1948**, 2240.
[25] K.-F. Tebbe, M. E. Essawi, S. A. E. Khalik, *Z. Naturforsch. B* **1995**, *50b*, 1429.
[26] A. J. Jircitano, M. C. Colton, K. B. Mertes, *Inorg. Chem.* **1981**, *20*, 890.
[27] a) F. H. Herbstein, M. Kapon, *J. Chem. Soc. Chem. Commun.* **1975**, 677; b) F. H. Herbstein, M. Kapon, *Philos. Trans. R. Soc. London A* **1979**, *291*, 199; c) F. H. Herbstein, M. Kapon, *Philos. Trans. R. Soc. London A* **1975**, 677.
[28] G. A. Landrum, N. Goldberg, R. Hoffmann, *J. Chem. Soc. Dalton Trans.* **1997**, 3605.
[29] a) R. D. Lowde, D. C. Phillips, R. G. Wood, *Acta Crystallogr.* **1953**, *6*, 553; b) F. H. Herbstein, G. M. J. Schmidt, *Acta Crystallogr.* **1955**, *8*, 399; c) D. C. Phillips, *Acta Crystallogr.* **1956**, *9*, 237; d) D. C. Phillips, F. R. Ahmed, W. H. Barnes, *Acta Crystallogr.* **1960**, *13*, 365.
[30] C. P. Brock, W. B. Schweizer, J. D. Dunitz, *J. Am. Chem. Soc.* **1991**, *113*, 9811.
[31] This type of interaction has recently been recognized as a typical supramolecular synthon for a wide range of nitrogen-containing aromatic solids: C. E. Marjo, M. L. Scudder, D. C. Craig, R. Bishop, *J. Chem. Soc. Perkin Trans. 2* **1997**, 2099.
[32] Y. Danten, B. Guillor, Y. Guissani, *J. Chem. Phys.* **1992**, *96*, 3795.
[33] T. W. Hanks, W. T. Pennington, R. D. Bailey in *Anisotropic Solids: Approaches to Polar Order* (Eds.: R. Glasier, P. Kaszynski), *ACS Symp. Ser.* **2000**, in press.
[34] a) F. Bigoli, P. Deplano, A. Ienco, C. Mealli, M. L. Mercuri, M. A. Pellinghelli, G. Pintus, G. Saba, E. F. Trogu, *Inorg. Chem.* **1999**, *38*, 4626; b) H. Tachikawa, E. Komatsu, *Inorg. Chem.* **1995**, *34*, 6546.
[35] a) G. C. Pimentel, *J. Chem. Phys.* **1951**, *19*, 446; b) R. J. Hach, R. E. Rundle, *J. Am. Chem. Soc.* **1951**, *73*, 5899.

Received: January 3, 2000 [F2222]